

⁵When all of the fast centers have the same correlation time, then N_{eff} equals the net number of acceptors, for our case. When there is a very great variation of τ among the centers, certain centers can predominate and N_{eff} must be specially evaluated, as will be seen for the hopping mechanism.

⁶For example, see Ko Sugihara, J. Phys. Soc. Japan **18**, 961 (1963).

⁷A. Miller and E. Abrahams, Phys. Rev. **120**, 745 (1960).

⁸Actually, because of the weak dependence of T_1 on

τ [see Eq. (3)], τ_h ranging even considerably beyond $0.1(\gamma_n H)^{-1}$ and $10(\gamma_n H)^{-1}$ will still contribute effectively to T_1 . However, the basic arguments do not change, and we will for simplicity continue to consider $\gamma_n H \tau_h(R) \sim 1$ as the criterion for effective relaxation.

⁹M. Pollak and T. H. Geballe, Phys. Rev. **122**, 1742 (1961).

¹⁰A. Abragam, Principles of Nuclear Magnetism (Clarendon Press, Oxford, England, 1961), pp. 390-391.

¹¹M. Gueron, Phys. Rev. **135**, A200 (1964).

PARAMAGNETIC HELICAL CURRENT FLOW IN TYPE-II SUPERCONDUCTORS*

M. A. R. LeBlanc, B. C. Belanger, and R. M. Fielding

Electronics Sciences Laboratory, University of Southern California, Los Angeles, California

(Received 1 March 1965; revised manuscript received 29 March 1965)

A charged particle q moving with nonzero components of velocity parallel and perpendicular to a uniform applied magnetic field H_a , and in zero electric field, will follow a helical trajectory. This helix can be described as diamagnetic, since the orbital circulation of q generates a magnetic field inside the orbit which opposes H_a . In this Letter we report on observations of an increase in the longitudinal flux threading type-II superconducting wires in an applied longitudinal field when a transport current is introduced in the specimen.^{1,2} This phenomenon, called the longitudinal paramagnetic effect, indicates that the current carriers in type-II superconductors follow paramagnetic helical trajectories.

The occurrence of a paramagnetic effect in type-I superconductors is well established,^{3,4} and has been shown to correlate with the restoration of resistance.⁵ In type-I superconductors, a paramagnetic helical current configuration is thought to arise because the specimen adopts an intermediate-state structure which maintains the field $B = H_c$ at the surface of the superconducting domains, and thereby provides least resistance along helical paths.^{3,4} In our samples no resistance is observed until the critical current is reached (where the onset of resistance is abrupt), whereas the paramagnetic effect first appears at currents considerably below I_c . Presumably, in the mixed state of type-II superconductors, paramagnetic helical trajectories are followed by the current because these minimize the Lorentz force exerted on the flux filaments.⁶

We present data obtained with (i) an as-received, severely cold-worked 0.025-cm-diameter Nb (25%) Zr Westinghouse wire with 0.007-cm-thick Cu cladding, and (ii) a 0.125-cm-diameter, high-purity Nb (50%) Ta M.R.C. wire annealed for 1 h at 1100°C and 10^{-8} Torr, yielding a resistivity ratio of ≈ 30 . Each wire is embedded in epoxy in a glass tube to ensure rigidity. The excess or deficit of longitudinal flux threading the wire is determined by ballistically monitoring the emf induced in a pickup coil surrounding the sample when the latter is thermally demagnetized⁷ (also at this juncture, $I \rightarrow 0$). To circumvent the problem of critical current limitation arising from contact Joule heating when $I > 250$ A in our samples, the section of the NbZr wire seen by the pickup coil was maintained at a suitable constant temperature higher than that of the 4.2°K bath.

The flux threading the samples depends not only on the final values of I , H , and T , but also is determined by the previous history of these variables. In this Letter we only present observations where the current is isothermally increased to its critical value after the sample has cooled through the critical temperature T_c in a constant applied longitudinal field H_a . Using this procedure we note that the longitudinal flux threading the sample increases as $I \rightarrow I_c$ and reaches a maximum at I_c .

Since it has been established that the critical current can be polarity dependent,⁸ the behavior of I_c and of the magnetization as $I \rightarrow I_c$ was investigated for each direction of current flow. Although we noted differences of a few percent

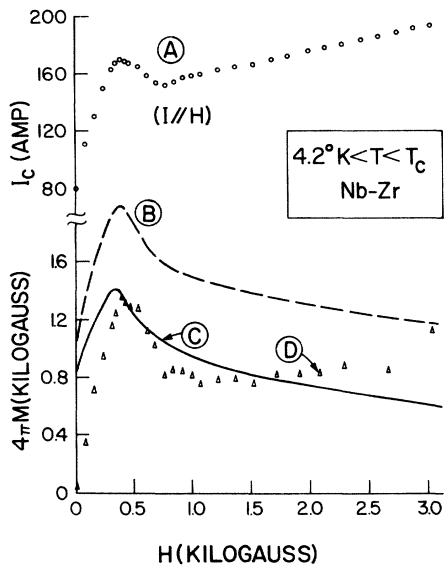


FIG. 1. Nb(25%)Zr wire, 0.025 cm diameter. Curve A: Critical current I_c versus applied longitudinal field. Curve B: Paramagnetic magnetization at I_c calculated from force-free model described in text. Curve C: Paramagnetic magnetization at I_c calculated from Meissner model described in text. Curve D: Paramagnetic magnetization at I_c when the transport current is introduced after cooling through T_c in constant longitudinal field.

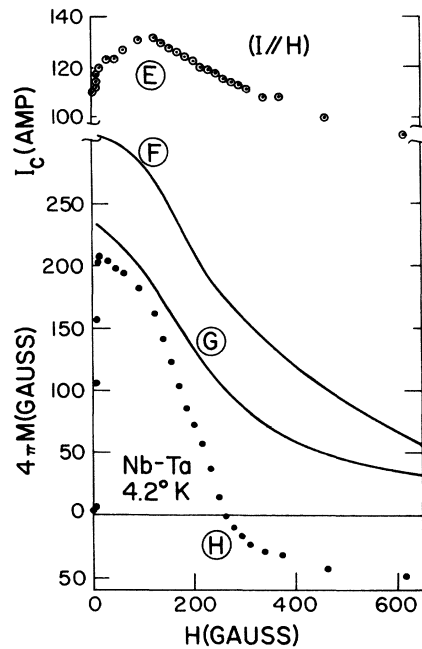


FIG. 2. Nb(50%)Ta wire, 0.125 cm diameter. Curve E: Critical current versus applied longitudinal field. Curve F: Paramagnetic magnetization at I_c calculated from force-free model. Curve G: Paramagnetic magnetization at I_c calculated from Meissner model. Curve H: Paramagnetic magnetization at I_c (previous history as in curve D of Fig. 1).

in the critical current and in the magnetization, dependent on the direction of current flow, in this Letter we present only results for current flowing in the direction of maximum I_c and the corresponding magnetization at I_c .

(i) NbZr wire.—Curve A of Fig. 1 gives I_c vs H_a . [The peak in I_c at low fields appears, more or less pronounced, in all the Nb(25%)Zr Wah Chang and Westinghouse wires we have studied.] Curve D of Fig. 1 shows $4\pi M(I_c)$, the magnetization at I_c . All data of Fig. 1 were obtained at the same temperature T_1 , where $T_1 \approx 8^\circ\text{K}$.

(ii) Nb-Ta wire.—Curves E and H of Fig. 2 show I_c and $4\pi M(I_c)$, respectively.

Figure 3 gives the initial magnetization at $I=0$ in increasing H_a (curve I) and the partial Meissner effect upon cooling in H_a (curve J). Curve K shows the flux-trapping behavior in decreasing field after cooling to 4.2°K at $H_a = 0.32$ kG. This procedure yields the maximum remanence at $H \approx 0$ in this sample. The magnetization data at I_c (curve H) are again presented for comparison. It can be seen that the maximum longitudinal flux in the wire at

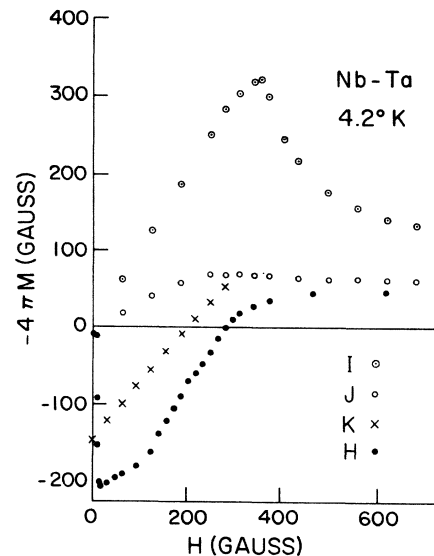


FIG. 3. Curve I: Magnetization in increasing longitudinal field ($I=0$). Curve J: Flux expulsion (Meissner effect) upon cooling in longitudinal field. Curve K: Magnetization in decreasing field after cooling at 0.32 kG. Decreasing field curves obtained from other previous histories lie above this one. Curve H: Reproduced from Fig. 2 for comparison.

I_c can be appreciably larger than the maximum remanence. Since the latter presumably represents a saturated critical state where the sample is filled with induced (Bean-type⁹) flux trapping currents at the critical density, the presence of more flux at I_c (when $H_a < 150$ G) is unexpected. The discussion presented later resolves this paradox.

In both samples, we note the correspondence between the initial rise in I_c vs H_a and the onset of the paramagnetic effect. This correlation extends over a wide range of applied fields in the Nb-Zr wire, whereas in the Nb-Ta sample it is sharp and appears when the total field at the surface of the wire is $\approx H_{c1}$. The initial rise of I_c versus longitudinal H_a observed in type-II superconductors has been attributed to the penetration of the applied field into the cross section of the wire and the accompanying change from superficial to bulk flow of current.¹⁰ Our observations show that this explanation is incomplete and that the initial increase in I_c is associated with the onset of the paramagnetic effect.

(A) Force-free model.—Since Bergeron¹¹ has shown that the large hump in I_c vs H_a observed in type-II superconductors¹² is consistent with a force-free (hence paramagnetic) transport current configuration, we attempt to interpret our results in terms of a simple version of this model. The force-free condition for an infinite cylinder can be given generally by $\vec{j}(\mathbf{r}) = f(B, r)\vec{B}(\mathbf{r})$, where $\vec{j}(\mathbf{r})$ is the current density and $\vec{B}(\mathbf{r})$ is the local field. For simplicity, we assume $f(B, r) = \alpha(H_T)$, where H_T is the total field at the surface of the wire. Introducing this condition in Maxwell's equation $\nabla \times \vec{B} = 4\pi\vec{j}$ in cylindrical coordinates for an infinite cylinder leads to the solutions¹³

$$B_z(r) = \alpha J_0(\alpha r) \text{ and } B_\theta(r) = \alpha J_1(\alpha r),$$

where $J_0(\alpha r)$ and $J_1(\alpha r)$ are Bessel functions of the first kind, and $z \parallel H_a$. From the definition of the longitudinal magnetization we obtain

$$4\pi M(I) \equiv \frac{2}{R^2} \int_0^R [B_z(r) - H_a] r dr = \frac{2I}{5\alpha R^2} - H_a,$$

where R = wire radius in cm and we have used $B_\theta(R) = I/5R$. We determine α at I_c from the experimental data and the relation $I_c/5RH_a = J_1(\alpha R)/J_0(\alpha R)$, where $\alpha R < 2.43$ (solutions with $\alpha R > 2.43$ are energetically unfavored). Curves *B* and *F* of Figs. 1 and 2, respective-

ly, give $4\pi M(I_c)$ obtained from this calculation. Although the poor agreement with our data can be attributed to the simple form assumed for $f(B, r)$, it is clear that any force-free model would only be applicable to ideal type-II superconductors, and for such samples we expect and observe better agreement with our simple model.

(B) Meissner model or nearly force-free configuration.—Since the longitudinal critical current is enhanced by the presence of suitable pinning regions,¹² Lorentz force effects should be taken into consideration in understanding the behavior of the paramagnetic effect and the critical current in nonideal type-II superconductors. We next proceed in this direction.

Meissner⁴ has derived an equation for the maximum paramagnetic moment in type-I superconductors which is in excellent agreement with the data in these materials.⁵ Although Meissner derived this equation from considerations of the intermediate state, by suitably modifying his assumptions we now obtain the same expression applicable to the mixed state. Following Meissner, we assume that (i) the longitudinal current density $j_z(r)$ is uniform throughout the specimen, hence $j_z(r) = 5B_\theta(R)/\pi R$ and $B_\theta(r) = (r/R)B_\theta(R)$ for an infinite cylinder, and (ii) $B_z^2(r) + B_\theta^2(r) = H_T^2 \equiv H_a^2 + (I/5R)^2$. This last assumption is more general than the condition postulated by Meissner⁴ and is equivalent to the requirement that the magnetic pressure $P_m \equiv \nabla(B^2) = 0$ throughout the specimen. The longitudinal magnetization is then given by

$$4\pi M(I) = \frac{2I}{15R} \left\{ \left[1 + \left(\frac{5RH_a}{I} \right)^2 \right]^{3/2} - \left(\frac{5RH_a}{I} \right)^3 \right\} - H_a.$$

Curves *C* and *G* of Figs. 1 and 2, respectively, show that $4\pi M(I_c)$ obtained from this relation is in satisfactory agreement with the data.

Several authors¹⁴ have shown that the critical-state magnetization of nonideal type-II superconductors can be separated into a reversible and an irreversible contribution. Druyvesteyn¹⁴ has shown in transverse fields that the irreversible part tends to vanish as $I - I_c$, while the reversible part persists. Presumably the change from paramagnetic to diamagnetic behavior in the Nb-Ta sample (curve *H*) can be attributed to this equilibrium diamagnetism.

We describe the Meissner model as nearly

force free since the angle $\theta(r) = \cos^{-1}(\vec{j} \cdot \vec{B})$ is always small ($\theta < 20^\circ$) and decreases as H_a increases. The resultant Lorentz force density

$$F_L(r) \equiv j_\theta B_z - j_z B_\theta = (-I^2/10\pi R^3)(r/R),$$

and is seen to be nonuniform and to be directed inward. In the paramagnetic effect, j_θ is positive, hence the Lorentz force experienced by the charged particles circulating around the wire axis is opposed by the force occurring when the particles acquire a longitudinal velocity. Therefore, higher azimuthal current densities can be sustained without exceeding the critical Lorentz force⁶ when a transport current is present, and the maximum longitudinal flux at I_C can exceed the maximum remanence (compare curves K and H of Fig. 3). Pursuing these considerations, we expect that (a) I_C' , the critical current at small fields when a remanent moment is trapped in the wire before I is applied, will exceed the critical current I_C observed with no excess flux initially present, and (b) I_C' will increase as the initial excess flux increases. These expectations are verified by our and other measurements.¹⁰

According to present views, flux threads type-II superconductors in the form of quantized filaments or current vortices¹⁵ which tend to align with their cores along \vec{B} . Our observations indicate that when a current near the critical value is present in cylindrical specimens in low longitudinal applied fields, the vortices should adopt a "paramagnetic" helical configuration with \vec{j} flowing along or nearly along the vortex cores. Presumably this configuration is assumed because it tends to minimize the total energy of the system when the pressure arising from the Lorentz force and transmitted to the flux filaments is taken

into account.

It is a pleasure to acknowledge the stimulating interest and suggestions of Dr. F. L. Vernon, Jr., in this work, and the assistance of C. C. Perkins in the calculations.

*Research supported by the U. S. Atomic Energy Commission.

¹B. C. Belanger, R. M. Fielding, and M. A. R. LeBlanc, *Bull. Am. Phys. Soc.* **9**, 713 (1964).

²M. W. Williams and C. J. Bergeron, Jr., *Bull. Am. Phys. Soc.* **10**, 60 (1965).

³W. Meissner, F. Schmeissner, and H. Meissner, *Z. Physik* **130**, 521, 529 (1951); **132**, 529 (1952); *Phys. Rev.* **90**, 709 (1953).

⁴H. Meissner, *Phys. Rev.* **97**, 1627 (1955); **101**, 31 (1956).

⁵J. C. Thompson, *Phys. Rev.* **102**, 1004 (1956); *J. Phys. Chem. Solids* **1**, 61 (1956).

⁶P. W. Anderson and Y. B. Kim, *Rev. Mod. Phys.* **36**, 39 (1964).

⁷S. H. Goedemoed, A. Van der Giessen, D. De Klerk, and C. J. Gorter, *Phys. Letters* **3**, 250 (1963); M. A. R. LeBlanc, *Phys. Rev. Letters* **11**, 149 (1963).

⁸M. A. R. LeBlanc, *Phys. Letters* **8**, 226 (1964).

⁹C. P. Bean, *Phys. Rev. Letters* **8**, 250 (1962).

¹⁰G. D. Cody and G. W. Cullen, *RCA Rev.* **25**, 466 (1964).

¹¹C. J. Bergeron, Jr., *Appl. Phys. Letters* **3**, 63 (1963).

¹²S. T. Sekula, R. W. Boom, and C. J. Bergeron, Jr., *Appl. Phys. Letters* **2**, 102 (1963). J. W. Heaton and A. C. Rose-Innes, *Phys. Letters* **9**, 112 (1964); *Cryogenics* **4**, 85 (1964).

¹³H. P. Furth, M. A. Levine, and R. W. Waniek, *Rev. Sci. Instr.* **28**, 949 (1957).

¹⁴P. S. Swartz, *Phys. Rev. Letters* **9**, 448 (1962); J. Silcox and R. W. Rollins, *Rev. Mod. Phys.* **36**, 52 (1964); W. A. Fietz, M. R. Beasley, J. Silcox, and W. W. Webb, *Phys. Rev.* **136**, A335 (1964); W. F. Druyvesteyn, *Phys. Letters* **14**, 275 (1965).

¹⁵A. A. Abrikosov, *Zh. Eksperim. i Teor. Fiz.* **32**, 1442 (1957) [translation: *Soviet Phys.-JETP* **5**, 1174 (1957)].